Electronic Supplementary Material (ESI) for Green Chemistry.

Regio- and Stereo-Selective Amination of Fatty Acids to D-Amino Acids by a Three-Step One-Pot Cascade

Xing Yu,[a] Xin-Yi Chen,[a] Hui-Lei Yu,[a] Jian-He Xu[a] and Zhi-Jun Zhang*[a]

X. Yu, X. Y. Chen, Prof. H. L. Yu, Prof. J. H. Xu, Dr. Z. J. Zhang
State Key Laboratory of Bioreactor Engineering, Shanghai Collaborative Innovation Centre for Biomanufacturing, East China University of Science and Technology, Shanghai 200237, China
E-mail: zjzhang@ecust.edu.cn

Table of Contents

1. Experimental Procedures

1.1. Chemicals

All chemicals were purchased from commercial sources. Hexanoic acid and L-norleucine were obtained from Shanghai Macklin Biochemical Co., Ltd. (Shanghai, China). Racemic-2-hydroxyhexanoic acid and D-norleucine were obtained from Aladdin Chemistry Co., Ltd. (Shanghai, China). 2-Oxohexanoic acid were purchased from Shanghai Haohong Biomedical Technology Co., Ltd. (Shanghai, China). All other chemicals and reagents were obtained from authentic suppliers at least of reagent grade and used without further purification.

1.2. Biocatalysts

1.2.1. Cloning, expression and purification of P450 peroxygenases

$P450_{CLA}$ from *Clostridium acetobutylicum* (GenBank accession number: WP_034583258.1).
$P450_{Jα}$ from *Jeotgalicoccus* (GenBank accession number: WP_198687604.1).
$P450_{SPα}$ from *Sphingomonas paucimobilis* (GenBank accession number: WP_017980797.1).
The genes encoding $P450_{CLA}$, $P450_{Jα}$ and $P450_{SPα}$ were synthesized after codon optimization against *E. coli* using the OptimumGene algorithm, inserted into pET-28a(+) plasmid by GenScript (Nanjing, China), and subsequently expressed in *E. coli* BL21 (DE3) cells. For heterologous expression, cells were grown overnight (180 rpm, 37°C) in a test tube containing 4 mL lysogeny broth (LB) medium supplemented with 50 μg/mL kanamycin as preculture. For protein expression, 6 mL of pre-culture was transferred into 600 mL TB medium in a 2 L shake flask supplemented with 50 μg/mL kanamycin and 600 μL of filter sterilized trace elements solution and incubated at 180 rpm and 37°C. At an optical density (OD_{600}) of 0.8, the expression was induced by adding 0.2 mM (final concentration) IPTG (isopropyl β-D-1-thiogalactopyranoside) and 0.5 mM (final concentration) δ-aminolevulinic acid (ALA). After incubation for another 20 h at 25°C, the cells were harvested by centrifugation (8000 × *g*, 10 min) at 4°C. Cells were resuspended in 20 mL purification buffer A (KPi, 100 mM, pH 7.5, 100 mM KCl and 10 mM imidazole), and disrupted by ultrasonication (15 min at 30% amplitude; 4 sec on, 6 sec off). Cell debris was removed by ultracentrifugation (13000 × *g*, 45 min, 4°C). The supernatant was filtered through a sterile 0.45 μm filter (Jingteng, China) to eliminate residual particles, and loaded onto a Ni NTA Beads 6FF column (Changzhou, Jiangsu). For purification, the column was washed with 20 mL buffer A, and $P450_{CLA}$ was eluted by buffer B (KPi, 100 mM, pH 7.5, 100 mM KCl and 500 mM imidazole). The fraction containing $P450_{CLA}$ (~20 to 40 mL) was exchanged with imidazole-free buffer C (KPi, 100 mM, pH 7.5, 100 mM KCl) to remove residual imidazole using an Ultrafiltration centrifuge tube (Millipore, 30 kDa) at 4°C. Both the activity and concentration of the enzyme were measured via analysis of reduced CO difference spectra as described by Omura and Sato.[1]
The expression and purification of $P450_{Jα}$ and $P450_{SPα}$ were the same with $P450_{CLA}$, unfortunately, the purification of $P450_{SPα}$ was because it's mainly expressed as inclusion bodies (Fig. S1). Both $P450_{CLA}$ and $P450_{Jα}$ were successfully purified using the above procedure (Fig. S2).

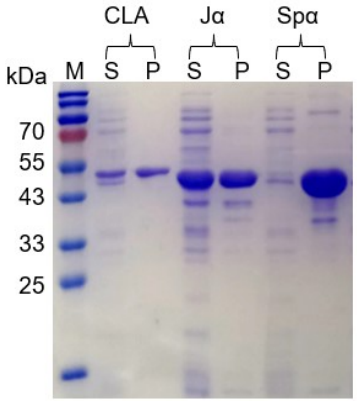

Fig. S1. SDS-PAGE analysis of the expression levels of $P450_{CLA,}$ $P450_{Jα}$ and $P450_{SPα}$. S: supernatant of cell lysate, P: precipitate of cell lysate, M: protein marker.

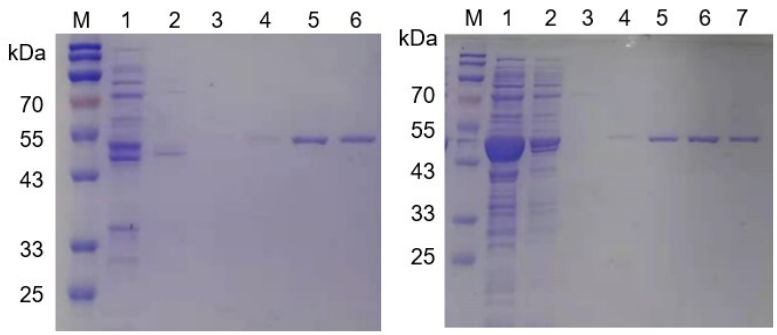

Fig. S2. 12.5% SDS-PAGE analysis of P450. a) $P450_{CLA}$. Lane 1: supernatant of cell lysate, Lane 2: flow-through, Lane 3-4: washing fractions, Lane 5-6: elution fractions. b) $P450_{Jα}$. Lane 1: supernatant of cell lysate, Lane 2: flow-through, Lane 3-4: washing fractions, Lane 5-7: elution fractions. M: protein marker.

1.2.2. Cloning, expression and purification of α-hydroxyacid oxidases

(*R*)-α-HAO from *Gluconobacter oxydans* (GenBank accession number: AAW61807.1).
(*S*)-α-HAO from *Aerococcus viridans* (GenBank accession number: 4RJE_A).
The genes encoding (*R*)-α-HAO and (*S*)-α-HAO were ordered (GenScript, Nanjing, China) after codon optimization against *E. coli*. (*R*)-α-HAO was inserted into pETDuet-1 using restriction sites *EcoR*I and *Hind*III to bear a His6-tag. (*S*)-α-HAO was cloned into pET-28a(+) using restriction sites *Nco*I and *Xho*I to bear a His6-tag. Both (*R*)-α-HAO and (*S*)-α-HAO were expressed in *E. coli* BL21 (DE3) cells. The expression of (*R*)-α-HAO and (*S*)-α-HAO was induced with 0.2 mM (final concentration) IPTG at 16°C and 180 rpm for 20 h. The expression and purification procedures of (*R*)-α-HAO and (*S*)-α-HAO were similar to those of P450 peroxygenases. (*R*)-α-HAO and (*S*)-α-HAO were then purified and analyzed on SDS-PAGE (Fig. S3).

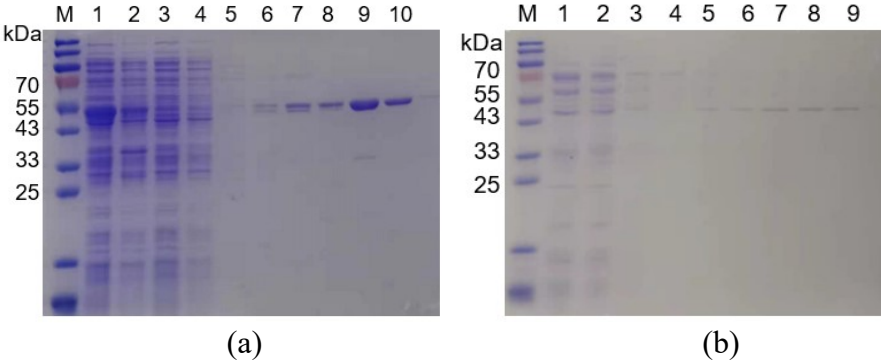

Fig. S3. 12.5% SDS-PAGE analysis of HAO. a) (*R*)-α-HAO. Lane 1: supernatant of cell lysate, Lane 2: precipitate of cell lysate, Lane 3: flow-through, Lane 4-6: washing fractions, Lane 7-10: elution fractions, b) (*S*)-α-HAO. Lane 1: supernatant of cell lysate, Lane 2: precipitate of cell lysate, Lane 3: flow-through, Lane 4-6: washing fractions, Lane 7-9: elution fractions, M: protein marker.

1.2.3. Cloning, expression and purification of *Ut*DAADH

*Ut*DAADH from *Ureibacillus thermosphaericus* (GenBank accession number: 5GZ3_A).
The gene encoding *Ut*DAADH was synthesized (GenScript, Nanjing, China) after codon optimization and inserted into pET-28a(+) using restriction sites *Ned*I and *Xho*I to bear a His6-tag. The recombinant plasmid was subsequently transformed into *E. coli* BL21 (DE3) cells for enzyme expression.
For overexpression of *Ut*DAADH, the recombinant *E. coli* cells were inoculated into 4 mL lysogeny broth (LB) with 50 μg/mL kanamycin at 37°C, 200 rpm for 10 to 12 h. Then 1 mL of preculture was inoculated to 100 mL LB medium in shake flask containing 50 μg/mL kanamycin and incubated at 37°C, 200 rpm for about 2 to 3 h until OD_{600} reached 0.6 to 0.8, followed by addition of IPTG to a final concentration of 0.2 mM. After cultivation at 16°C, 200 rpm for another 20 h, the cells were harvested by centrifugation (13,000 × *g*, 5 min, 4°C), resuspended in purification buffer A (pH 8.0, 20 mM Tris, 250 mM NaCl, 10 mM imidazole), and disrupted with an ultrasonic oscillator (JY92-II; Scientz Biotech Co.). The cell debris was then removed by centrifugation (13,000 × *g*, 45 min, 4°C). The supernatant was loaded onto a Ni NTA Beads 6FF column (Changzhou, Jiangsu), which was previously equilibrated with purification buffer A. The Ni-NTA column was then treated with 50 mM imidazole (pH 8.0) for 5 column volumes to remove the contaminated protein and 5 column volumes buffer B (pH 8.0, 20 mM Tris, 250 mM NaCl, 500 mM imidazole) to elute the target protein, respectively. The solution containing target protein was concentrated and desalted with an ultrafiltration tube (Millipore, 10 kDa) at the same time by purification buffer C (pH 8.0, 25 mM Tris, 150 mM NaCl) until the volume of the solution was less than 1 mL, then the pure enzyme was stored at -80°C for further use. SDS-PAGE results of purification of *Ut*DAADH were shown in Fig. S4.

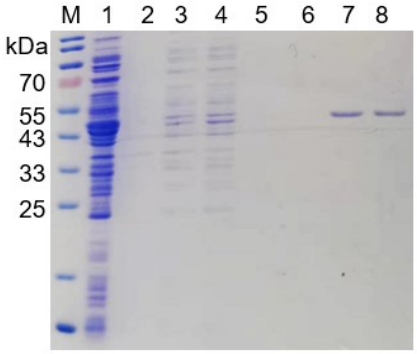

Fig. S4. 12.5% SDS-PAGE analysis of *Ut*DAADH. Lane 1: supernatant of cell lysate, Lane 2: precipitate of cell lysate, Lane 3: flow-through, Lane 4-6: washing fractions, Lane 7-8: elution fractions. M: protein marker.

1.2.4. Lyophilization of *Ut*DAADH

The expression of *Ut*DAADH was induced with 0.2 mM (final concentration) IPTG at 16°C and 180 rpm for 20 h. After that, the cells were harvested via centrifugation (13,000 × *g*, 5 min, 4°C). For preparation of the lyophilized cell-free extract, the cells were resuspended in potassium phosphate buffer (10 mM, pH 7.0) and then disrupted by high-pressure homogenization, and after centrifugation (13,000 × *g*, 45 min, 4°C) the supernatant of cell lysate was freeze-dried for 72 h. The lyophilized enzyme powder was stored at 4°C for further use.

1.3. Activity assay of purified enzymes

1.3.1. $P450_{CLA}$

The activity of purified $P450_{CLA}$ was determined for the oxidation of **1a** (Scheme S1). The oxidation reactions were performed in 500 µL scale in a 2 mL micro-centrifuge tube at 20°C, 1000 rpm for 24 h. The reaction solution was extracted with EtOAc containing 0.05% (v/v) 1-decanol as internal standard, then derivatized (details see section 1.4.4) and analyzed by GC or GC-MS.
Reaction mixtures contained 5 mM **1a**, 10% (v/v) EtOH, 0.5 µM $P450_{CLA}$, 1 mM H_2O_2 and reaction buffer (KPi,100 mM, pH 7.5).
The specific activity (U/mg) of $P450_{CLA}$ toward **1a** was determined by a short reaction. Specific activity of $P450_{CLA}$ was determined as U per mg purified enzyme or as concentration of active protein in µM (determined by CO-titration). One unit of enzyme activity was defined as the amount of $P450_{CLA}$ required for the formation of 1µmol product in 1 min.

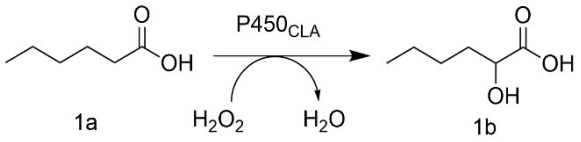

Scheme S1. Oxidation of 5 mM **1a** with $P450_{CLA}$.

1.3.2. (*R*)-α-HAO and (*S*)-α-HAO

Both the activities of purified (*R*)-α-HAO and (*S*)-α-HAO were determined for the oxidation of ***rac*-1b** (Scheme S2-S3). The oxidation reactions were performed in 500 µL scale in a 2 mL micro-centrifuge tube at 20°C, 1000 rpm for 24 h. The reaction solution was extracted with EtOAc containing 0.05% (v/v) 1-decanol as internal standard, then derivatized (details see section 1.4.4) and analyzed by GC or GC-MS. During GC analysis, we found that the product 2-oxo-hexanoic acid **1c** was easily transformed into its enol form **1e** (Scheme S4).
Reaction mixture with (*R*)-α-HAO contained 10 mM ***rac*-1b**, 10% v/v EtOH, 1.0 mg/mL (*R*)-α-HAO, 0.05 mg/mL catalase and reaction buffer (KPi, 100 mM, pH 7.5).
Reaction mixture with (*S*)-α-HAO contained 10 mM ***rac*-1b**, 10% v/v EtOH, 0.5 mg/mL (*S*)-α-HAO, 0.05 mg/mL catalase, 0.1 mM FMN and reaction buffer (KPi, 100 mM, pH 7.5).
The specific activity (U/mg) of (*R*)-α-HAO or (*S*)-α-HAO toward **(*R*)-1b** or **(*S*)-1b** was determined by a short reaction. One unit of enzyme activity was defined as the amount of (*R*)-α-HAO or (*S*)-α-HAO required for the depletion of 1 µmol substrate in 1 min.

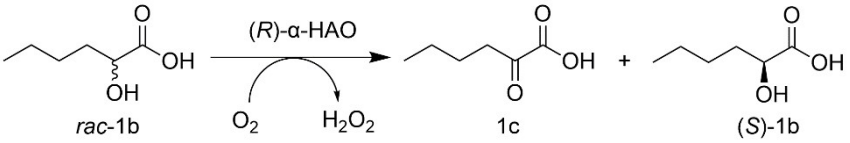

Scheme S2. Oxidation of 10 mM *rac*-1b with (*R*)-α-HAO (catalase was implemented to remove H_2O_2).

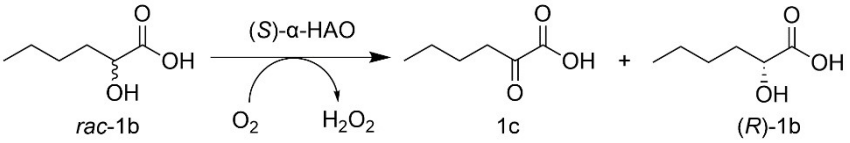

Scheme S3. Oxidation of 10 mM *rac*-1b with (*S*)-α-HAO (catalase was implemented to remove H_2O_2).

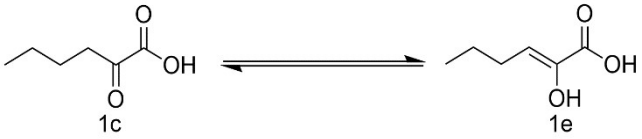

Scheme S4. Transformation of enol form for 1c.

1.3.3 *Ut*DAADH

The activity of *Ut*DAADH was measured in the oxidative deamination direction. The activity of *Ut*DAADH toward D-norleucine (**1d**) was detected at 50°C by monitoring the change of absorbance at 340 nm within 1 min on a UV-visible spectrophotometer (UV-1900i; Shimadzu Co.), which was caused by the reduction of $NADP^+$ to NADPH.
Reaction mixture (1 mL) contained 30 μL D-norleucine (15 mM), 10 μL $NADP^+$ (1 mM), 20 μL purified enzyme with appropriate dilution, and 940 μL glycine/NaOH buffer (200 mM, pH 9.0). One unit of enzyme activity was defined as the amount of *Ut*DAADH required for the formation of 1 μmol NADPH in 1 min. All experiments were conducted in triplicate.

1.4. Reaction design

1.4.1. Internal H_2O_2 recycling reaction

The continuous oxidation of **1a** to **1c** was performed by $P450_{CLA}$, (*R*)-α-HAO and (*S*)-α-HAO via an internal H_2O_2 recycling system (Scheme S5), which was first adopted by Kurt Faber et al. for the continuous oxidation of octanoic acid in 2018.[2]
The reaction mixture contained 5 μM $P450_{CLA}$, 10 mM **1a**, 10% EtOH (co-solvent), 0.1 mM FMN, 1 mg/mL (*R*)-α-HAO, 1 mg/mL (*S*)-α-HAO and H_2O_2 at different equivalents. Cascade reactions were performed in 500 μL scale in 2 mL micro-centrifuge tube. All reactions were performed in duplicate at 20°C and 1000 rpm for 12 h.

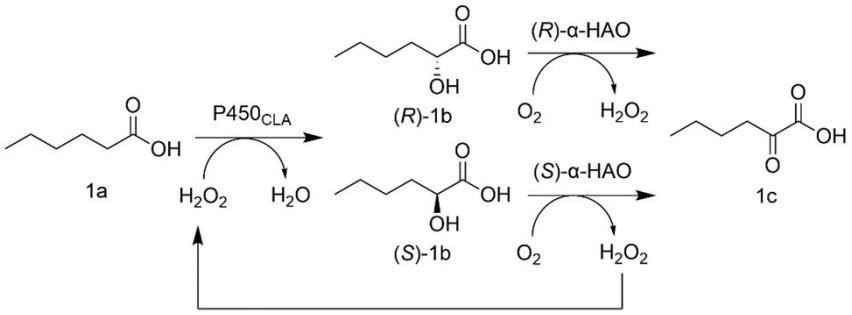

Scheme S5. Enzymatic oxidation of **1a** to **1c** with $P450_{CLA}$, (*R*)-α-HAO and (*S*)-α-HAO.

1.4.2. Internal NAPDH recycling reaction

Asymmetric reductive amination of **1c** to **1d** was realized by *Ut*DAADH and a formate dehydrogenase to recycle the expensive cofactor (Scheme S6).
The reaction mixture contained *Ut*DAADH and *Bst*FDH (1:1) at different enzyme activity (0.2~0.6 U/mL), 20 mM **1c** (5% v/v DMSO co-solvent), 0.1 mM NADPH and ammonium formate at various concentrations. All reactions were performed in duplicates under various conditions (temperature and pH).

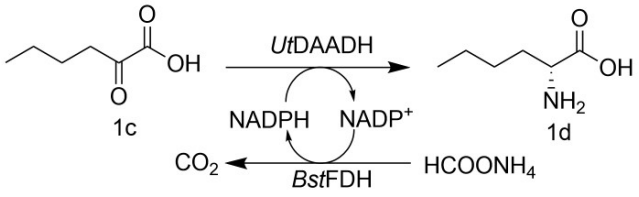

Scheme S6. Conversion of **1c** to **1d** by using the ammonium formate driven bioreaction.

1.4.3. One-pot three-step enzymatic cascade

Three-step one-pot conversion of **1a** to **1d** was performed by utilizing five enzymes ($P450_{CLA}$, (*R*)-α-HAO, (*S*)-α-HAO, *Ut*DAADH and *Bst*FDH) (Scheme S7).

The reaction mixtures contained 5 μM $P450_{CLA}$, 10/20 mM **1a**, 10% EtOH (co-solvent), 0.1 mM FMN, (*R*)-α-HAO at various concentrations (1~2 mg/mL), (*S*)-α-HAO at various concentrations (1~2 mg/mL), *Ut*DAADH and *Bst*FDH (1:1) at different enzyme activity (0.4~0.8 U/mL), 1 M $HCOONH_4$ and H_2O_2 at different equivalents. Cascade reactions were performed in 500 μL scale in 2 mL micro-centrifuge tube. All reactions were performed in duplicate at 20°C and 1000 rpm for 12 h or 24 h.

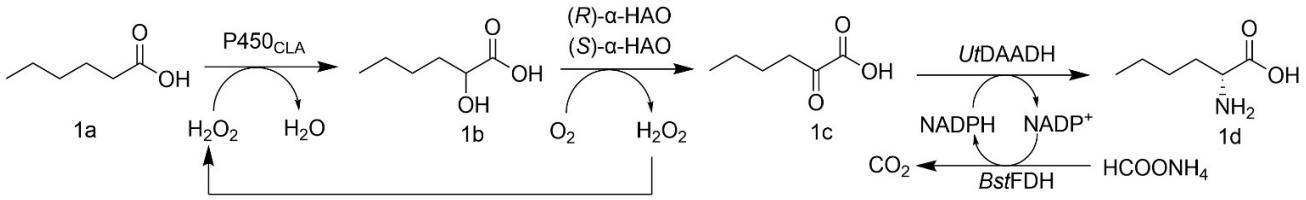

Scheme S7. Conversion of **1a** to **1d** by one-pot three-step enzymatic cascade.

1.4.4. General procedure for extraction and derivatization of reaction compounds for GC, GC/MS and HPLC analysis

Carboxylic acids (fatty acids, hydroxy acids, and oxo-acids) were analyzed by GC or GC-MS after methyl esterification. The reaction solution (500 μL scale) was quenched by the addition of 200 μL 1 N HCl. Substrates and products were extracted with 500 μL EtOAc containing 0.05% 1-decanol (v/v) as internal standard. The organic phase was collected and dried with anhydrous Na_2SO_4. Then 50 μL organic phase was mixed with 50 μL MeOH followed by supplementation of 10 μL 2 M TMSCHN2 (trimethylsilyl diazomethane in diethyl ether). After incubated at room temperature (RT) for 30 min, the sample was analyzed by GC or GC-MS directly.

Amino acid products were analyzed by HPLC after pre-column derivatization using a Marfey's reagent.[3] In the single step reaction catalyzed by *Ut*DAADH, reaction solution (500 μL scale) was quenched by the addition of 500 μL acetonitrile and then centrifuged to remove the protein precipitate, the supernatant was used as stock solution. In the cascade reaction, reaction solution (500 μL scale) was quenched by the addition of 200 μL 1 N HCl and 500 μL EtOAc was then used to extract the remaining carboxylic acids, after removing the organic phase, the aqueous phase was centrifuged to remove the protein precipitate. Finally, 280 μL supernatant was mixed with 120 μL acetonitrile and used as stock solution.

The general derivatization method is as follows: 20 μL of stock solution was mixed with 72 μL acetonitrile, 32 μL of 1 M sodium bicarbonate solution and 90 μL of 14 mM Marfey's reagent stock. The reaction mixture was vortexed, heated at 40 ºC for 1 h and cooled to room temperature. Then, 40 μL of 1 N HCl was added to quench the reaction. HPLC analysis was performed after filtrating the sample through a 0.22 μm filter.

1.4.5. GC and GC-MS analytical methods

After derivatization as described in **1.4.4**, the reaction samples were analyzed using a SHIMADZU Nexis GC-2030 system equipped with a flame ionization detector and SH-Rtx-1 column (30.0 m × 0.25 mm, 0.25 μm) using nitrogen as the carrier gas. Injector temperature: 280°C; injection volume: 1 μL; Split ratio 20:1; pressure 100 kPa; column temperature program: 80°C, hold for 1 min, 5°C min^{-1} to 90 °C, hold for 1 min, and 5°C min^{-1} to 95°C, hold for 6 min, and 25°C min^{-1} to 250°C, hold for 1 min. Retention times (min): methyl-1a, 3.8; methyl-1b, 5.5; methyl-1c, 8.1; internal standard (1-decanol), 13.4.

Chiral analysis of reaction samples was performed using a SHIMADZU GC-2014 system equipped with a flame ionization detector and an Agilent J&W CP-Chiralsil-DEX CB capillary column (25 m × 0.25 mm × 0.25 μm) using nitrogen as the carrier gas. Reaction samples of **1a**: Injector temperature 280°C; Split ratio 20:1; column temperature program: 85°C, hold for 2 min, 5°C min^{-1} to 90 °C, hold for 5 min, and 20°C min^{-1} to 100°C, hold for 5 min, and 25°C min^{-1} to 180°C, hold for 2 min. Reaction samples of **2a-5a**: Injector temperature 280°C; Split ratio 20:1; column temperature program: 90°C, hold for 2 min, 10°C min^{-1} to 100 °C, hold for 3 min, and 20°C min^{-1} to 120°C, hold for 3 min, and 25°C min^{-1} to 180°C, hold for 12 min.

GC-MS analysis was conducted on a GCMS-QP2010 SE (Shimadzu, Kyoto, Japan) instrument equipped with a HP-5MS column (30 m × 0.25 mm × 0.25 μm) using He as carrier gas. Injector temperature: 250°C; Split ratio 20:1; column temperature program: 80°C, hold for 2 min, 20°C min^{-1} to 100 °C, hold for 7 min, and 20°C min^{-1} to 250°C, hold for 3 min. EI mode, MS Source: 230 °C.

1.4.6. HPLC analytical methods

After derivatization as described in **1.4.4**, the analytic yield of product D-norleucine (**1d**) was determined using a high-performance liquid chromatography (HPLC) (Shimadzu) equipped with an Elite Hypersil ODS2 C18 column (250 mm × 4.6 mm, 5 μm). The following analytic conditions and retention times (RTs) were used: methanol: water 70:30, containing 0.1%(v/v) TFA, with a flow rate of 0.6 mL/min and detection at 320 nm, oven temperature 30°C, RT-**1d** = 12.5 min. For the analysis of **2d-5d**, the analytic conditions and

retention times (RTs) were used: methanol: water 75:25, containing 0.1%(v/v) TFA, with a flow rate of 0.6 mL/min and detection at 320 nm, oven temperature 30°C, RT-**2d** = 11.9 min; RT-**3d** = 15.7 min; RT-**4d** = 21.8 min; RT-**5d** = 31.2 min.

2. Results and Discussion

2.1. Activity assay for the purified enzymes

2.1.1. $P450_{CLA}$ and $P450_{J\alpha}$

The active concentration of $P450_{CLA}$ and $P450_{J\alpha}$ was determined by CO difference spectra (Fig. S5), both active concentration of $P450_{CLA}$ and $P450_{J\alpha}$ were calculated to be 20-30 µM. After determining the active concentration of $P450_{CLA}$ and $P450_{J\alpha}$, their hydroxylation activity towards **1a** were then evaluated. The reaction was performed in 500 µL scale containing KPi buffer (100 mM, pH 7.5), 5 mM 1a, $P450_{CLA}$ (1 µM) or $P450_{J\alpha}$ (4 µM), 5 mM H_2O_2 (0.5 mM H_2O_2 was supplemented every 30 min).
Successful formation of **1b** from **1a** was confirmed for $P450_{CLA}$ by GC analysis, while no product formation was observed for $P450_{J\alpha}$ (Fig. S6). To verify whether $P450_{J\alpha}$ was inactivated during storage, we tested its activity using the natural substrate lauric acid. The results showed that $P450_{J\alpha}$ was active on lauric acid, therefore we can conclude that $P450_{J\alpha}$ might not be able to hydroxylate fatty acids with shorter chain lengths. Based on these results, $P450_{CLA}$ was selected as the catalyst for the first step in the cascade. Furthermore, we calculated the specific activity of $P450_{CLA}$ towards **1a** as described in **1.3.1**, giving a specific activity of 0.22 ~ 0.37 U/mg (Table S1).

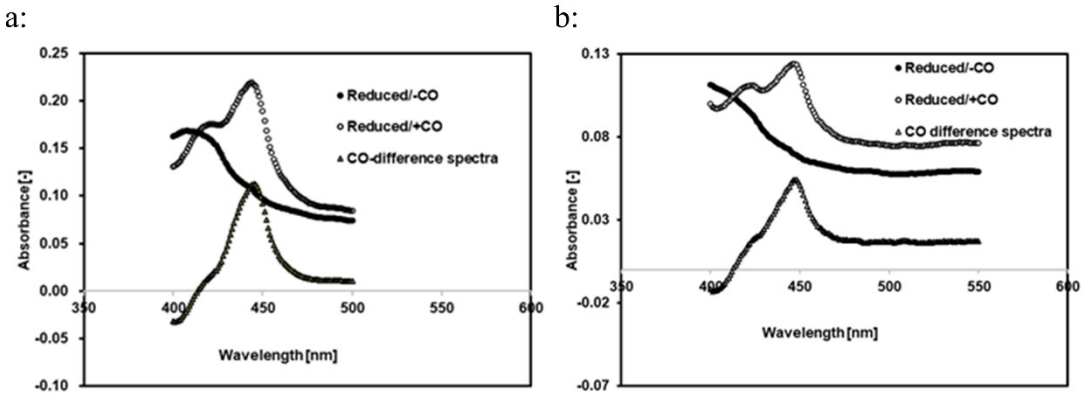

Fig. S5. CO difference spectra of purified a) $P450_{CLA}$, b) $P450_{J\alpha}$.

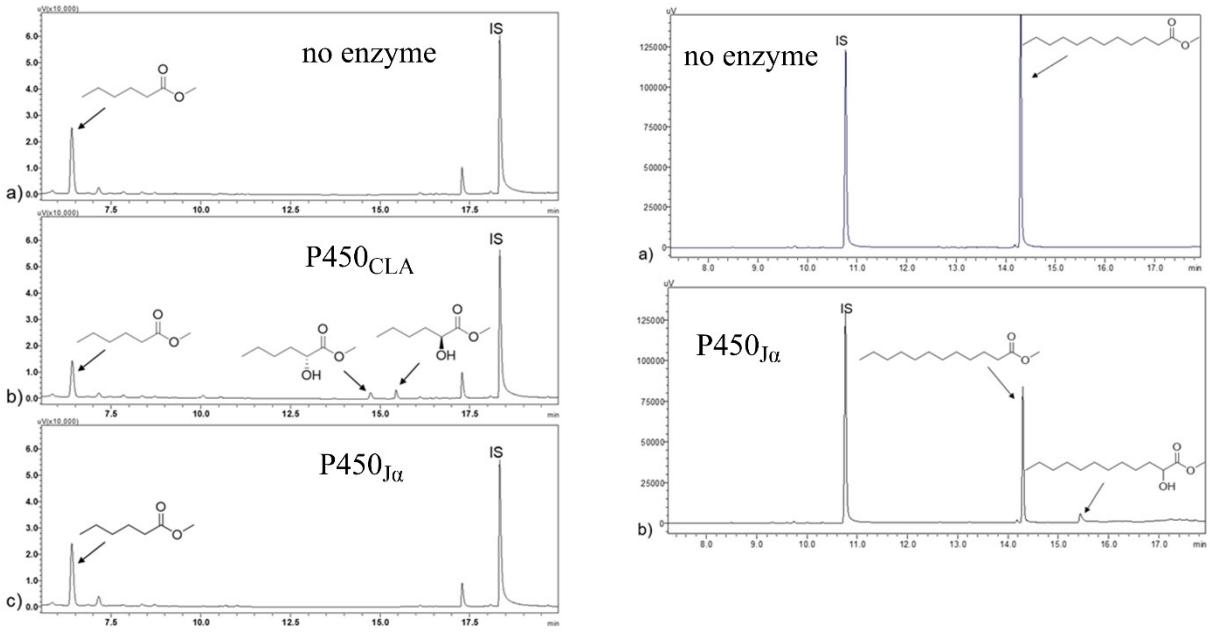

Fig. S6. Chiral GC chromatogram (left) for the oxidation of **1a** and achiral chromatogram (right) for the oxidation of lauric acid by P450.

Table S1. Specific activity of $P450_{CLA}$ towards **1a**.

Entry	Time [min]	H_2O_2 [mM]	1b [mM]	C[a] [%]	U/mg
1	10	1	0.092 ± 0.017	9.2	0.37
2	20	1	0.135 ± 0.000	13.5	0.27
3	30	1	0.164 ± 0.000	16.4	0.22

[a] coupling efficiency: mol product/mol H_2O_2.

2.1.2. (*R*)-α-HAO and (*S*)-α-HAO

The oxidase activity of purified hydroxy acid oxidases ((*R*)-α-HAO and (*S*)-α-HAO) was measured for the oxidation of ***rac*-1b** (Scheme S2-S3). Chiral GC analysis showed that both (*R*)-α-HAO and (*S*)-α-HAO have obvious activity and high preference for (*R*)-1b and (*S*)-1b, respectively (Fig. S7). It should be noted that the 2-oxo-hexanoic acid (1c) could be spontaneously transformed into its enol isomer reversibly (Scheme S4), giving cis/trans isomer of the enol product. The specific activity of (*R*)-α-HAO and (*S*)-α-HAO towards **1b** were calculated to be 37 mU/mg and 48 mU/mg, respectively.

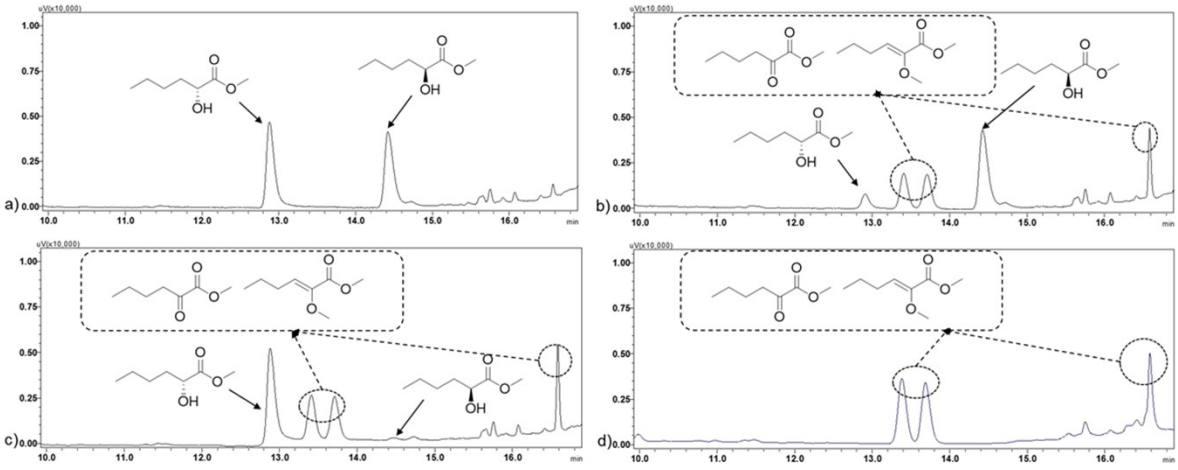

Fig. S7. Chiral GC chromatogram for the oxidation of 10 mM ***rac*-1b** with a) no enzyme, b) (*R*)-α-HAO (1.0 mg/mL), c) (*S*)-α-HAO (0.5 mg/mL), d) commercial standard of **1c**.

2.1.3. *Ut*DAADH

The specific activity of *Ut*DAADH on **1d** was measured as described in **1.3.3**. The specific activity of purified *Ut*DAADH towards D-norleucine (**1d**) was calculated to be 2.0 U/mg. Since lyophilized cell free lysate was used for the subsequent experiments, we also tested the activity of the lyophilized cell free lysate of *Ut*DAADH, which was calculated to be 0.77 U/mg. Commercial standard **1d** and the product from the reductive amination of 1c catalyzed by *Ut*DAADH were analyzed by HPLC after derivatization according to **1.4.4**. The results indicated that D-norleucine was exclusive produced with an *ee* of >99% (Fig. S8).

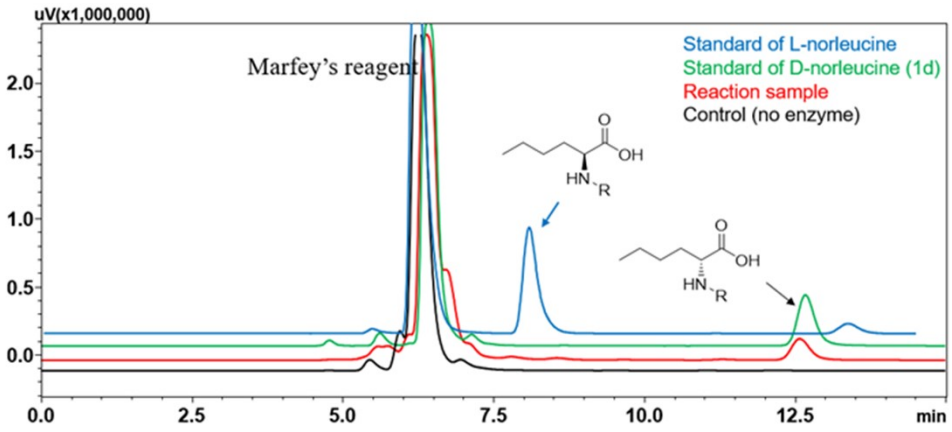

Fig. S8. HPLC chromatogram of D-norleucine (**1d**) produced by *Ut*DAADH.

2.2. Optimizing the reaction

2.2.1 Testing continuous oxidation reaction by using $P450_{CLA}$/(*R*)-α-HAO/(*S*)-α-HAO

2.2.1.1 Optimization of $P450_{CLA}$ loadings and substrate concentrations

To maximize the conversion of **1a** to **1b**, the reaction catalyzed by $P450_{CLA}$ needs to be performed efficiently. To choose the appropriate method of H_2O_2 addition, we compared the product formation by adding H_2O_2 at single mode and fed-batch mode (Table S2). The reaction mixture contained 2.5 μM $P450_{CLA}$, 5 mM **1a** ,5 or 10 mM H_2O_2 (using different addition modes). After 12 h reaction, both **1b** and **1c** were detected on GC due to overoxidation of **1b** (Fig. S9) and their corresponding concentrations were calculated by standard calibration curves.

The product formation of single addition mode was lower than fed-batch supplementation (pulsing 0.1 mol equivalent ever 30 min; totally 1 mol equivalent). In the case of singe addition mode (totally 1 or 2 mol equivalent of H_2O_2), the efficiency of H_2O_2-utilization was also significantly reduced. From the above data, it is clear that high concentrations of H_2O_2 indeed impair the catalytic activity of $P450_{CLA}$, and spontaneous decomposition of H_2O_2 is also present. In subsequent experiments, stepwise addition of 0.1 mol equivalent H_2O_2 was selected to maximize the product formation.

To investigate the total amount of H_2O_2 required to maximize the conversion of substrate, we monitored the time course for the conversion of **1a** (Fig. S10). The results showed that **1b** and **1c** were produced almost at the same trend, and the maximum concentrations of both products were obtained when totally 2 mol equivalent H_2O_2 were used (Table S3). Then fed-batch supplementation mode (pulsing 0.1 mol equivalent H_2O_2 every 30 min, totally 2 mol equivalent) was chosen for further investigation. Finally, 5 μM $P450_{CLA}$ was used for the conversion of 5 mM and 10 mM **1a** under previous conditions (Table S3).

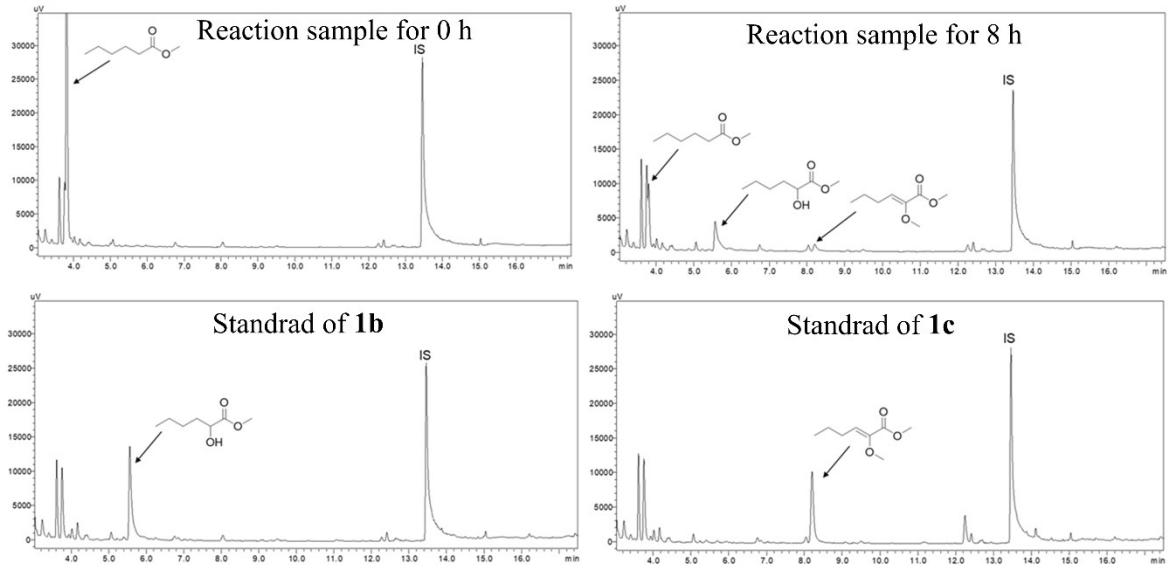

Fig. S9. Achiral GC analysis for the oxidation of **1a** to **1b** using $P450_{CLA}$.

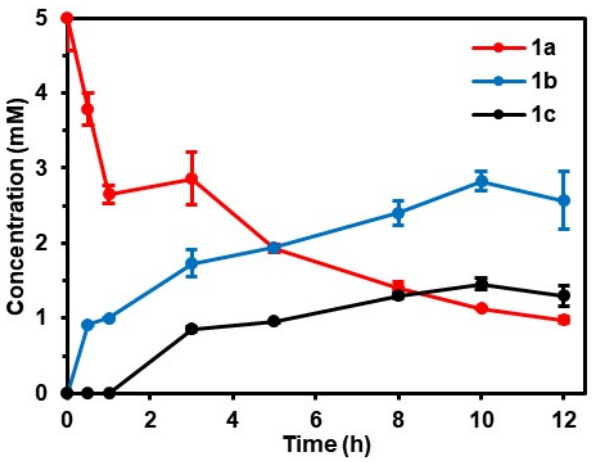

Fig. S10. Time profile for the conversion of 5 mM **1a**.

Table S2. Comparison of coupling efficiency of H_2O_2 between one-time addition and fed-batch addition of stoichiometric quantities of H_2O_2.

Entry	H_2O_2 [mM]	1b [mM]	1c [mM]	Conv. [a] [%]
1	5	1.13 ± 0.03	0.70 ± 0.02	36.6
2	10	1.56 ± 0.01	1.02 ± 0.04	51.6
3	2.5 + 2.5	1.12 ± 0.07	0.70 ± 0.01	36.4
4	1 + 1 × 4	1.32 ± 0.10	0.74 ± 0.02	41.2
5	0.5 + 0.5 × 9	1.90 ± 0.08	0.82 ± 0.02	54.4

[a] Conversion: (mol 1b + mol 1c)/mol substrate.

Table S3. Comparison of coupling efficiency and product formation under various conditions.

Entry	1a [mM]	Time [h]	H_2O_2 [mM]	1b [mM]	1c [mM]	C[a] [%]	Conv.[b] [%]
1	5	5	5	1.94 ± 0.01	0.96 ± 0.00	77.2	58.0
2	5	8	8	2.40 ± 0.16	1.30 ± 0.04	62.5	74.0
3	5	10	10	2.83 ± 0.13	1.46 ± 0.08	57.5	85.8
4	5	12	12	2.57 ± 0.38	1.30 ± 0.14	43.1	77.4
5	5[c]	10	10	2.63 ± 0.59	1.82 ± 0.21	62.7	89.0
6	10[c]	12	24	4.95 ± 0.00	2.89 ± 0.11	44.7	78.4

[a] Coupling efficiency: (mol 1b + 2 × mol 1c)/mol H_2O_2.

[b] Conversion: (mol 1b + mol 1c)/mol 1a.

[c] 5 μM $P450_{CLA}$ was used.

2.2.1.2. Testing continuous oxidation reaction via internal H_2O_2 recycling

By coupling $P450_{CLA}$ with (*R*)-α-HAO and (*S*)-α-HAO, an internal recycling of oxidant (H_2O_2) was developed, in which H_2O_2 produced from oxidation of hydroxy acids by (*R*)/(*S*)-α-HAO could then be utilized by $P450_{CLA}$ for the hydroxylation of fatty acids. Theoretically, only catalytic amount of H_2O_2 would be enough to launch the reaction, which would significantly simplify the process operation. The internal H_2O_2 recycling reaction was performed under the following conditions: KPi (100 mM, pH 7.5), 10 mM **1a**, 5 μM $P450_{CLA}$, 1 mg mL^{-1} (*R*)-α-HAO, and 1 mg mL^{-1} (*S*)-α-HAO, 0.1 mM FMN and different catalytic amounts of H_2O_2. All reactions were performed on 500 μL scale, 20°C, 12 h (Table 2 and Fig. S11).

To further improve the turnover number of H_2O_2, we also investigated the conversion level by subdividing 0.2 equivalent H_2O_2 into two separately portions (the first 0.1 equivalent H_2O_2 was added at 0 h, then the second 0.1 equivalent H_2O_2 portion was added after 5 h). As shown in Fig. S12, the conversion level of double 0.1 equivalent H_2O_2 addition was significantly higher than single 0.2 equivalent H_2O_2 addition. Therefore, we chose the double 0.1 equivalent H_2O_2 addition mode in the subsequent one-pot three-step cascade. Apart from **1a**, we also tested the internal H_2O_2 recycling cascade using other chain lengths fatty acids under the same condition (Fig. S13).

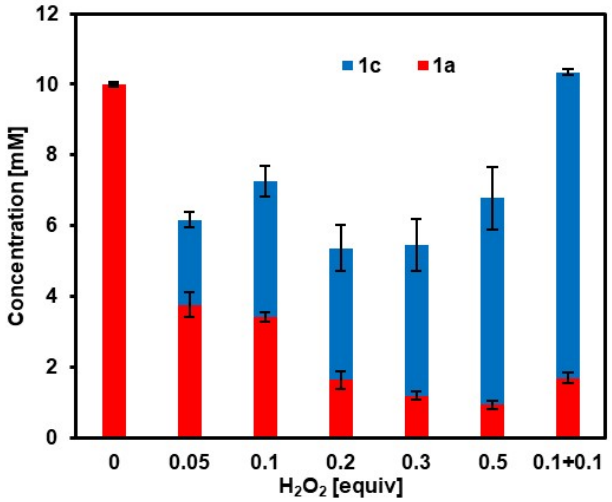

Fig. S11. Conversion of **1a** to **1c** with various H_2O_2 addition**.**

[a]. Hydroxy acid (**1b**) was not detected on GC, conversions were calculated by the formation of oxoacid (**1c**).

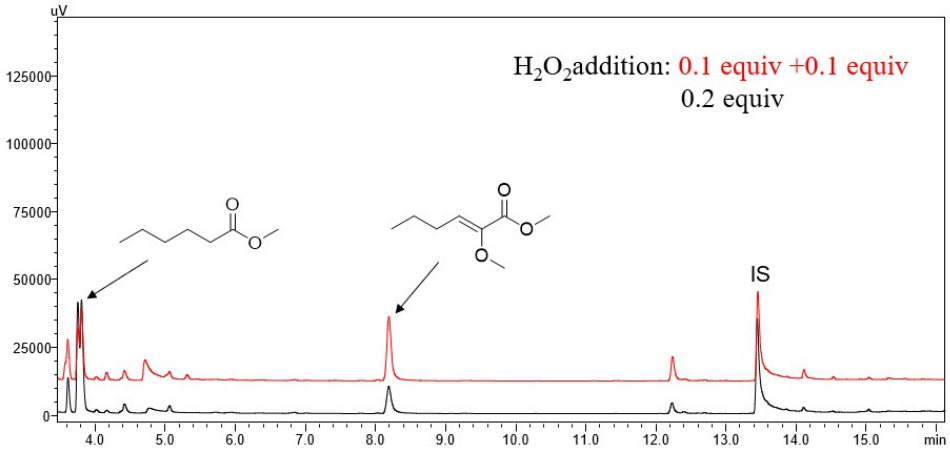

Fig. S12. Comparison of the conversion levels of **1a** to **1c** at different H_2O_2 addition modes.

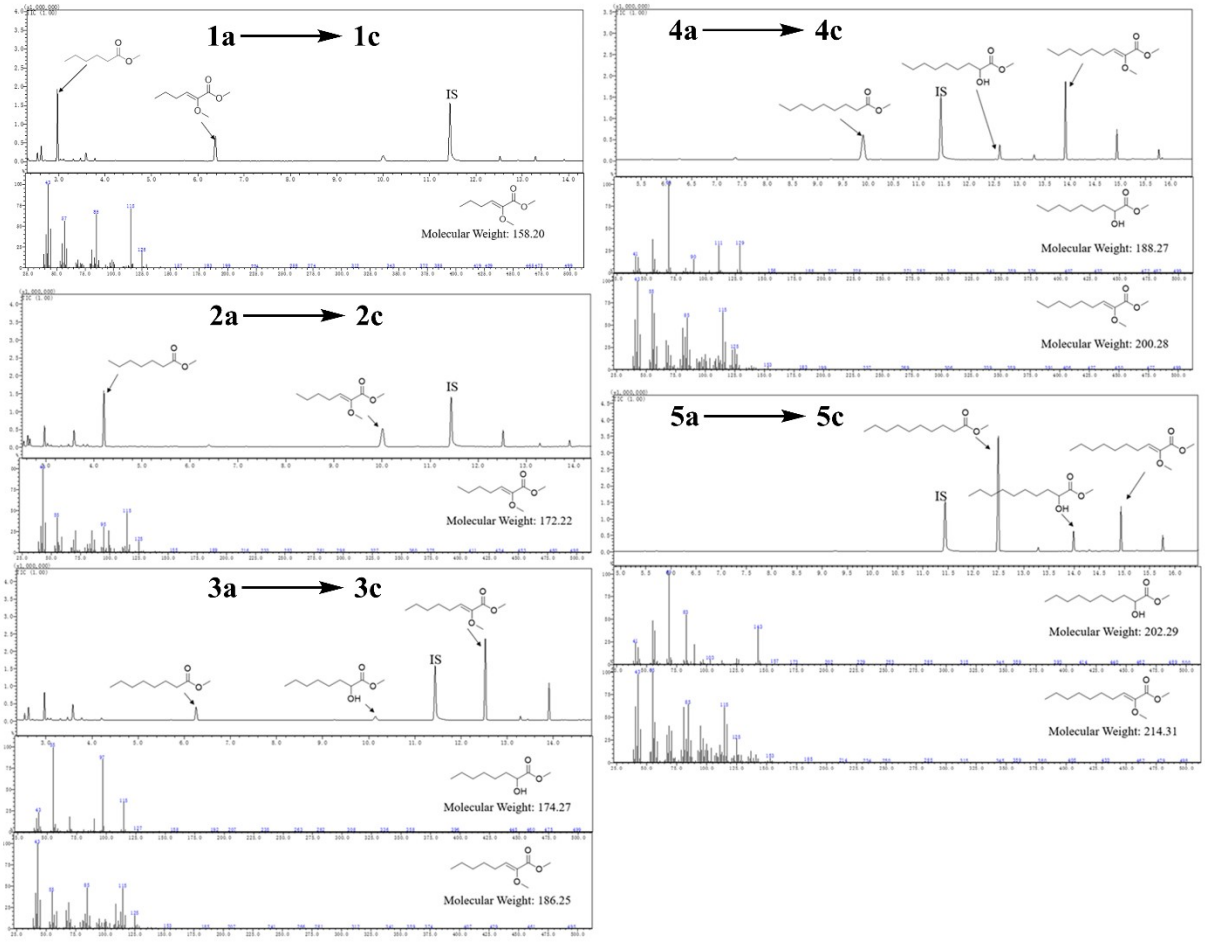

Fig. S13. GC-MS analysis for the conversion of 10 mM different chain lengths fatty acids by $P450_{CLA}$, (*R*)-α-HAO and (*S*)-α-HAO.

2.2.2. Testing asymmetric reductive amination by using *Ut*DAADH/*Bst*FDH

2.2.2.1. Optimization of the concentrations of *Ut*DAADH and *Bst*FDH, reaction temperatures, pH, and concentrations of ammonium formate

In order to convert **1c** obtained from continuous oxidation of **1a** into the target product **1d** as much as possible. Firstly, we tested the enzyme activity required to convert 20 mM **1c**. Reactions were performed under the following conditions: $HCOONH_4$-$NH_3.H_2O$ buffer (100 mM, pH 9.0), 20 mM **1c**, 0.2~0.6 U/mL *Ut*DAADH, 0.1 mM NADPH. We kept the ratio of the enzyme activity of *Ut*DAADH and *Bst*FDH to be 1:1 to ensure constant NADPH recycling. Then we monitored the reaction progress for 22 h. According to the time course (Fig. S14a), when the enzyme dosage was 0.2 U/mL, the reaction approached the end point in about 12 h. While when the enzyme dosage was increased to 0.4 U/mL and 0.6 U/mL, the reaction rate was significantly enhanced and the reaction end point was reached earlier, but the final product concentration was basically the same. Increasing the amount of enzyme could not increase the concentration of the product. As a result, 0.4 U/mL was considered as the optimal enzyme loading for the conversion of 20 mM **1c**. The effects of reaction temperature (20 ~ 60°C), buffer pH (7 ~ 9.5), and ammonium formate concentration (100 ~ 1000 mM) on the synthesis of D-norleucine (**1d**) were investigated with 0.4 U/mL enzyme loading. Reaction conditions were described in **1.4.2**. As shown in Fig. S14b, the highest conversion rate (91.3%) was obtained at 30°C. In order to compare the effect of different pH, we shortened the reaction time to 2 hours, and higher conversion efficiency was observed between pH 7 and 8 (Fig. S14c). Finally, as shown in Fig. S14d, 20 mM substrate could be completely transformed when the concentration of ammonium formate was 1 M. As a result, under the optimum transformation conditions (0.4 U/mL *Ut*DAADH, 0.4 U/mL *Bst*FDH, 30°C, KPi (100 mM, pH 7.5), 1 M ammomium formate), 20 mM 2-oxohexanoic acid (**1c**) could be completely converted into D-norleucine (**1d**).

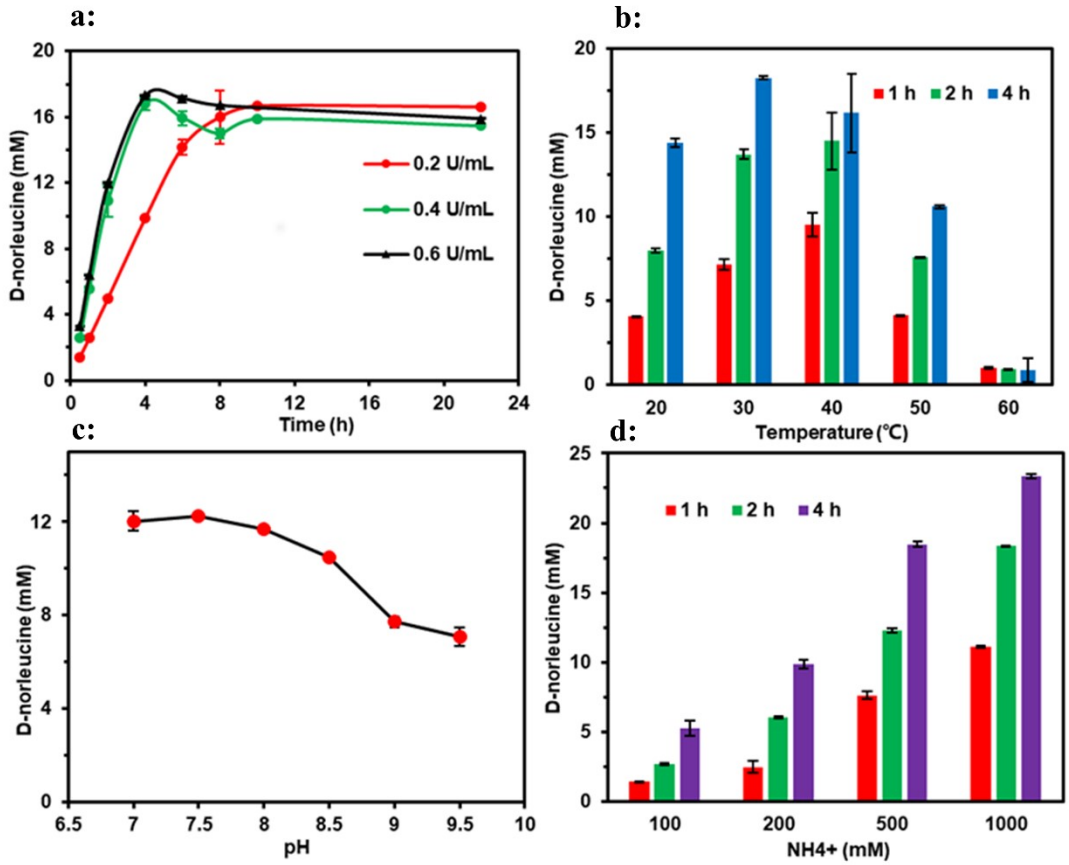

Fig. S14. **Reaction conditions optimization of *Ut*DAADH for the reductive amination of 2-oxohexanoic acid** (**1c**): a) enzyme dosage; b) reaction temperature; c) buffer pH; d) concentration of ammonium formate.

2.2.3. Testing the three-step one-pot enzymatic cascade

2.2.3.1 Testing the three-step one-pot cascade at different substrate, enzyme loadings and temperatures

The three-step one-pot cascade was first performed under the following conditions: KPi (100 mM, pH 7.5), 10 mM **1a**, 10% (v/v) EtOH, 5 μM $P450_{CLA}$, 1 mg mL^{-1} (*R*)-α-HAO, 1 mg mL^{-1} (*S*)-α-HAO, 0.4 U mL^{-1} *Ut*DAADH, 0.4 U mL^{-1} *Bst*FDH, 0.1 mM NADPH, 0.1 mM FMN, 1 M $HCOONH_4$, totally 0.2 equivalent H_2O_2 (0.1 equiv added at 0 h, another 0.1 equiv added at 5 h). All reactions were conducted in duplicate at 20°C and 1000 rpm.

The results indicated that **1a** was almost completely consumed and the formation of **1d** could reach up to 90%. Given the spontaneous decomposition of H_2O_2, the complete depletion of **1a** indicating that the added H_2O_2 was recycled at least 5 times throughout the cascade. The recycling efficiency of cofactor NADPH was efficient since the intermediate **1c** was not detected during the whole reaction. Then the same setups were tested with 0.5 equivalent H_2O_2 added at one time, but the conversion level was slightly lower than that of fed-batch mode (Fig. S15a). We also tested the formation of product **1d** at different substrate concentrations under the same conditions for 24 h (Table S4). To explore whether the conversion level of catalyzing 20 mM substrate could be further improved, we first monitored the progress under above optimized conditions (Fig. S15b). To further improve the formation of product **1d**, we optimized the activity ratio of HAO and DAADH, and the conversion levels were compared after reaction for 8 h (Fig. S15c).

The temperature effect on the cascade reaction was investigated. All reactions were performed on 500 μL scale, containing 20 mM **1a**, 10% (v/v) EtOH, KPi (100 mM, pH 7.5) and 5 μM $P450_{CLA}$, 74 mU mL^{-1} (*R*)-α-HAO, 96 mU mL^{-1} (*S*)-α-HAO, 800 mU mL^{-1} *Ut*DAADH, 800 mU mL^{-1} *Bst*FDH, 0.1 mM NADPH, 0.1 mM FMN, 1 M $HCOONH_4$, totally 0.2 equivalent H_2O_2 (0.1 equivalent H_2O_2 was added at 0 h, and the other 0.1 equivalent H_2O_2 was added at 5 h). All reactions were performed in duplicate, 1000 rpm, 12 h (Fig. S15d). To demonstrate the possible poor stability and activity of (*S*)-α-HAO, the conversion of 20 mM **(*S*)-1b** by different amounts of (*S*)-α-HAO at 15 ° C and 30 ° C, respectively, was also investigated. The conversion rate was calculated based on substrate consumption (Fig. S15e).

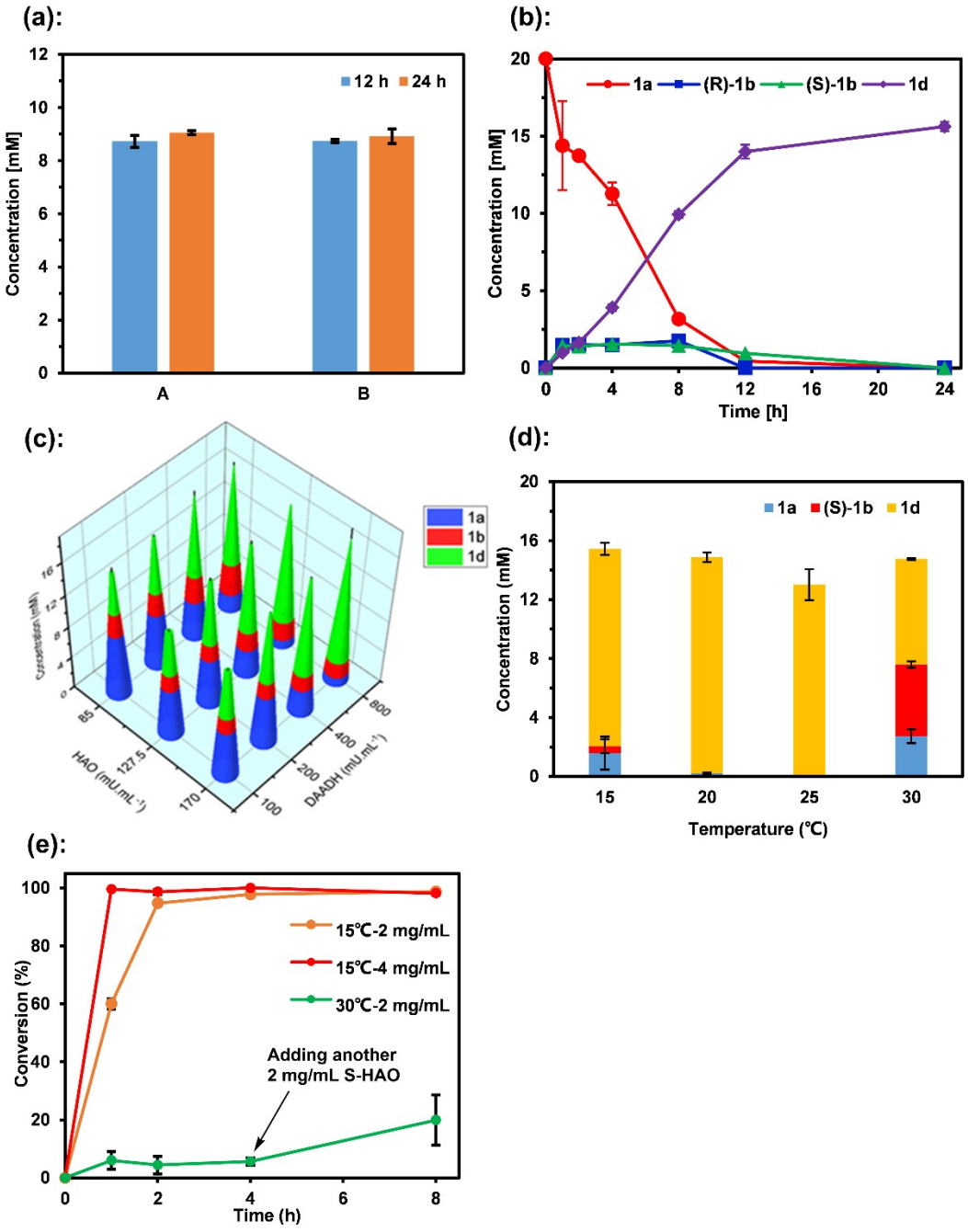

Fig. S15. **Three-step one-pot cascade catalyzed by P450$_{CLA}$, (*R*)-α-HAO and (*S*)-α-HAO, *Ut*DAADH, *Bst*FDH.** (a) Comparison of the conversion of 10 mM **1a** to **1d** with different H_2O_2 addition modes. A: double 0.1 equivalent H_2O_2; B: single 0.5 equivalent H_2O_2; (b) Time profile for the conversion of 20 mM **1a** to **1d**; (c) Effect of different activity ratio of HAO and DAADH on the formation of product **1d**; (d) Conversion of 20 mM **1a** to **1d** at different temperatures; (e) Conversion of 20 mM **(*S*)-1b** by different amounts of (*S*)-α-HAO at different temperatures.

Table S4. Enzymatic conversion of various concentrations of **1a** to **1d** via internal H_2O_2 and NADPH recycling in a one-pot three-step cascade.

Entry	1a [mM]	1d [mM]	Conv. [%]	$TON_{H_2O_2}$ (product)
1	10	9.06 ± 0.07	90.6	4.5
2	20	15.62 ± 0.31	78.1	3.9

3	50	19.37 ± 0.25	38.7	1.9

2.3. Conversion of different chain lengths fatty acids in the cascade

2.3.1. Effect of pH on the generation of C-1 truncated D-amino acid

Fatty acids with different chain lengths (C_6-C_{10}) were used as substrates in the cascade. Besides the expected product, a small new product peak was also observed by HPLC with all the substrates tested, and the new product was confirmed to be C1-truncated D-amino acid by comparing with commercial standards (Fig. S16). Previous studies have shown that 2-keto acids are prone to be decarboxylated to C1-truncated fatty acids at the presence of H_2O_2[4]. H_2O_2-mediated oxidative decarboxylation of α-ketoacids was then studied with 10 mM **1c**. As shown in Table S5, when H_2O_2 (> 2 mM) was incubated with **1c**, **1c** rapidly decomposed to pentanoic acid (Fig. S18). We speculate that H_2O_2-mediated decarboxylation of 2-keto acids leads to the generation of C1-truncated fatty acids, which are then converted into the corresponding D-amino acids by cascade (Scheme S8). Furthermore, it is also reported that pH is important for the rate of decarboxylation of α-ketoacids[5]. Therefore, we then performed the cascade under different pH conditions using **2a** as substrates. We found that at pH close to 8.0, the C1-truncated D-amino acid was significantly reduced (Fig. S19).

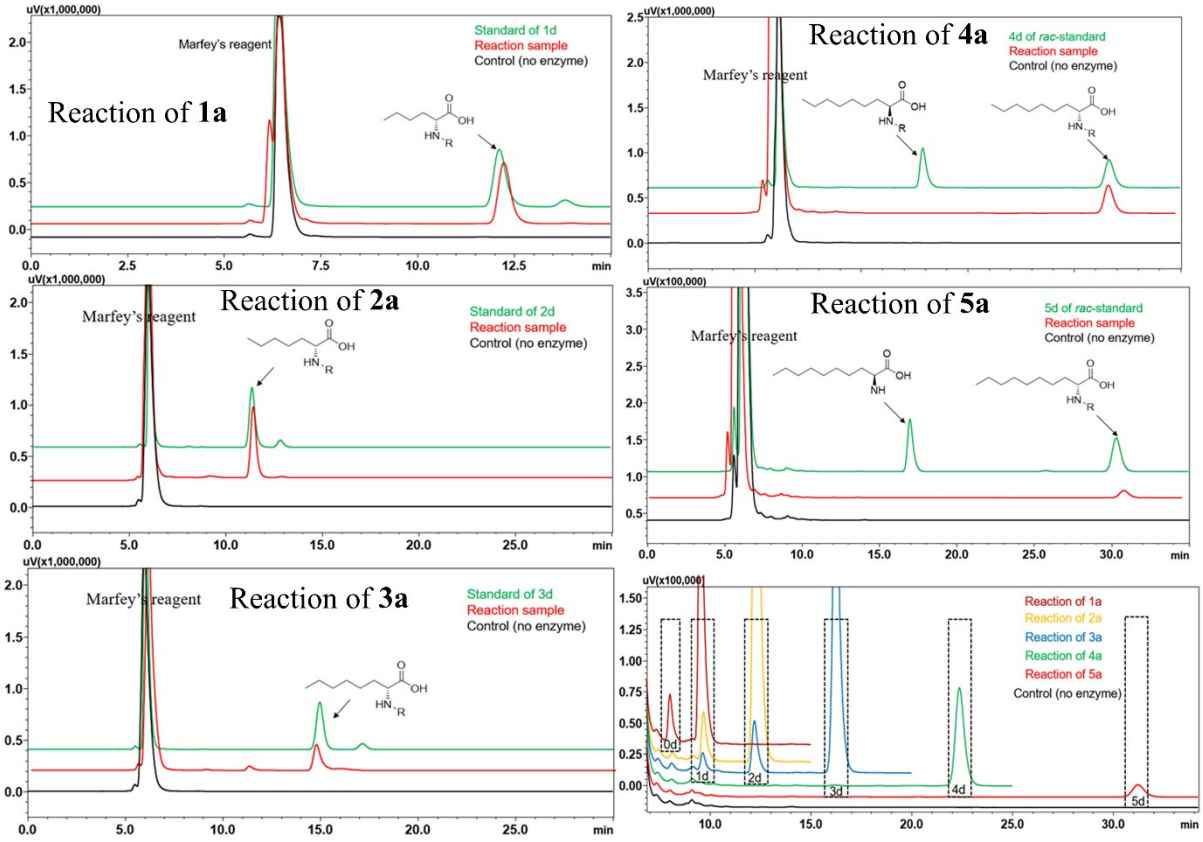

Fig. S16. HPLC analysis for the formation of D-amino acids via the cascade reactions using different fatty acids substrate.

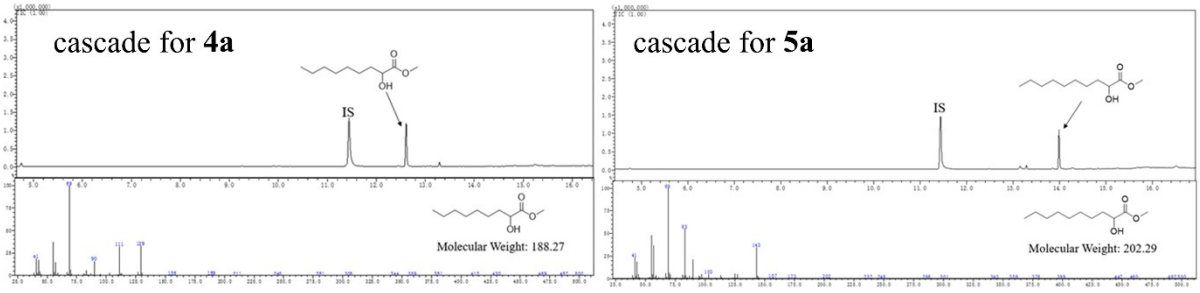

Fig. S17. GC-MS analysis of conversion of 10 mM **4a** or **5a** by three-step one-pot cascade after 24 h.

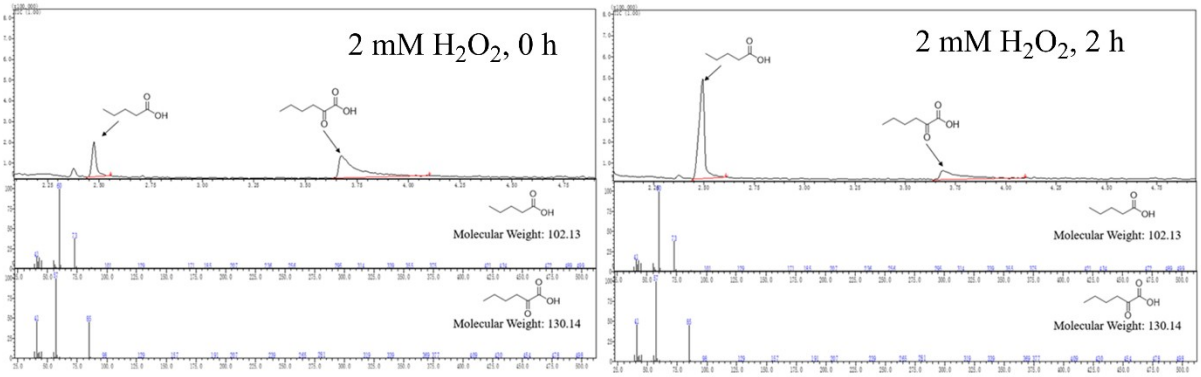

Fig. S18. GC-MS analysis of H_2O_2-mediated oxidative decarboxylation of 10 mM **1c**.

Table S5. Recovered 2-oxohexanoixc acid (10 mM **1c**) from reaction with H_2O_2 at different time points.

H_2O_2 [mM]	0	0.5	1	2	4	10
Time [h]						
0	10[a]	9.0	9.0	7.8	7.9	6.3
2	7.3	6.2	5.5	3.8	0.4	0
4	7.4	6.0	5.4	3.6	0.3	0

[a] The content of **1c** at 0 h without H_2O_2 was defined as 10 mM.

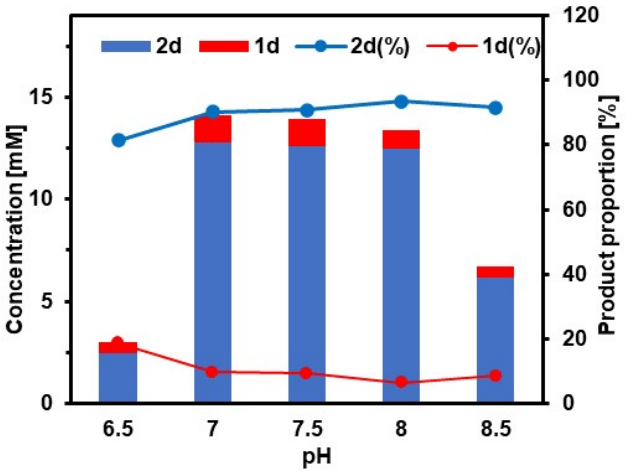

Fig. S19 Conversion of **2a** to **2d** at different pHs.

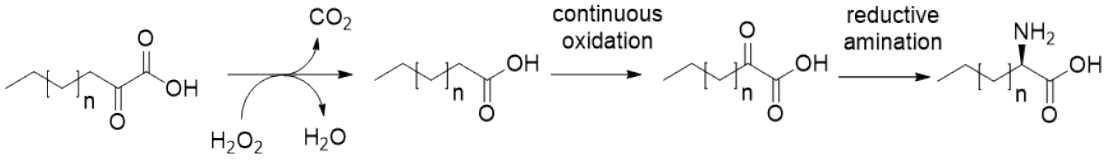

Scheme S8. Proposed synthetic route for C-1 truncated D-amino acid formation.

2.4. Preparation of D-amino acids by the cascade on semi-preparative scale

The three-step one-pot cascade was conducted on a semi-preparative scale using hexanoic acid (**1a**), heptanoic acid (**2a**) and octanoic acid (**3a**) as substrates. Reactions were performed on 35 mL scale containing KPi buffer (100 mM, pH 8.0), 10 mM substrate, 10%

EtOH, 5 μM $P450_{CLA}$, 74 mU mL^{-1} (*R*)-α-HAO, 96 mU mL^{-1} (*S*)-α-HAO, 800 mU mL^{-1} *Ut*DAADH, 800 mU mL^{-1} *Bst*FDH, 0.1 mM NADPH, 0.1 mM FMN, 1 M $HCOONH_4$, totally 0.2 equivalent H_2O_2 (0.1 equivalent was added at 0 h, and the other 0.1 equivalent H_2O_2 portion was added at 5 h) ‧ 20°C ‧ 200 rpm for 24 h.

Finally, the reaction was ceased by adding 37% HCl until pH 1.0 and the denatured proteins and insoluble particles were removed by centrifugation (10,000 × *g*, 30 min). The supernatant was collected and the pellet was resuspended in 10 mL MeOH, the supernatant was gathered after centrifugation (10,000 × *g*, 30 min). The supernatant was lyophilized for 24 h and then the resulting residue was dissolved in 0.1 M HCl solution. Amino acids were purified via ion exchange chromatography using HZ011 gel type cationic resin (Shanghai Huazhen Technology Co., Ltd, 100-200 mesh). The resin was pretreated by washing with 1 M HCl (3 × column volumes), and H_2O until the pH reached 6.0, then 1 M NaOH (3 × column volumes) and H_2O until the pH was 10, finally 1 M HCl (5 × column volumes). After the D-amino acid sample was loaded onto the resin, the column was washed with H_2O (10 × column volumes) to remove the uncombined compounds. Target amino acids were eluted with 2 M $NH_3.H_2O$. The fractions containing the target amino acid were detected by TLC or HPLC, combined and freeze-dried to remove residue $NH_3.H_2O$. Finally, 40.1 mg **1d** (87.4% isolated yield), 34.2 mg **2d** (67.2% isolated yield) and 30.4 mg **3d** (54.5% isolated yield) were obtained from 10 mM substrate. All the products were confirmed by ^1H NMR (Fig. S20, 22 & 24) and ^{13}C NMR (Fig. S23, 25 & 27).

1d: ^1H NMR (600 MHz, D_2O) δ 4.04 – 3.93 (m, 1H), 1.95 – 1.76 (m, 2H), 1.36 – 1.20 (m, 4H), 0.79 (t, *J* = 6.9 Hz, 3H). ^{13}C NMR (151 MHz, D_2O) δ 172.15, 52.76, 29.28, 26.09, 21.43, 12.82.

2d: ^1H NMR (600 MHz, D_2O) δ 4.00 (t, *J* = 6.3 Hz, 1H), 1.94 – 1.75 (m, 2H), 1.40 – 1.17 (m, 6H), 0.84 – 0.70 (m, 3H). ^{13}C NMR (151 MHz, D_2O) δ 172.14, 52.79, 30.30, 29.52, 23.59, 21.45, 13.07.

3d: ^1H NMR (600 MHz, D_2O) δ 3.98 (t, *J* = 6.3 Hz, 1H), 1.94 – 1.75 (m, 2H), 1.41 – 1.11 (m, 8H), 0.75 (d, *J* = 6.7 Hz, 3H). ^{13}C NMR (151 MHz, D_2O) δ 172.14, 52.78, 30.48, 29.55, 27.74, 23.86, 21.72, 13.21.

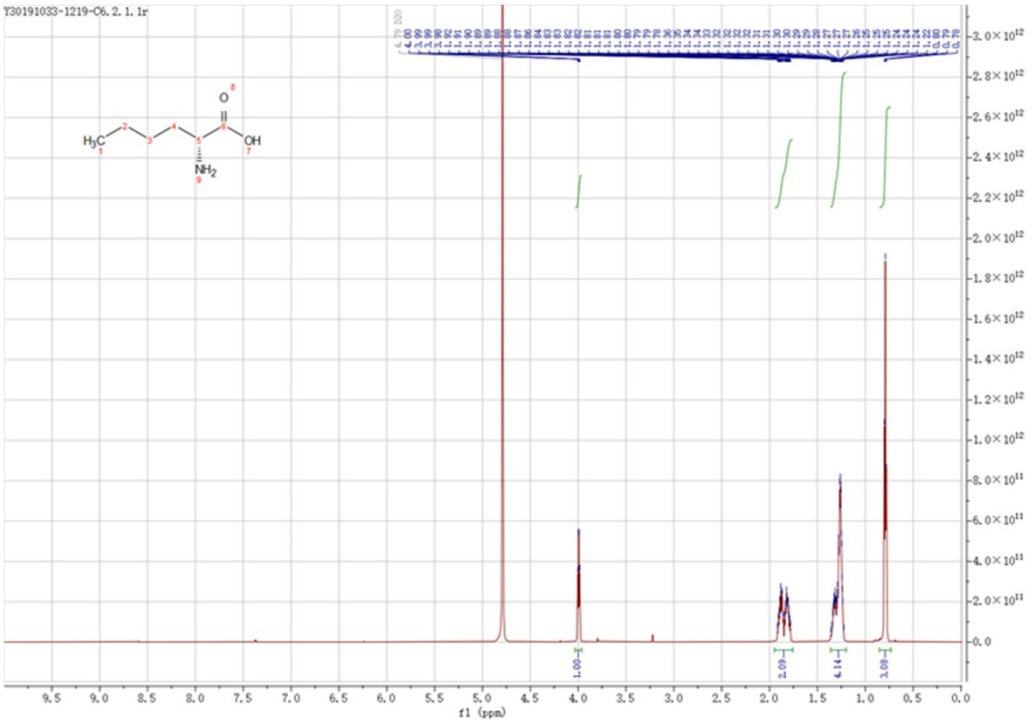

Fig. S20. ^1H NMR of isolated **1d** obtained from conversion of 10 mM **1a** by cascade.

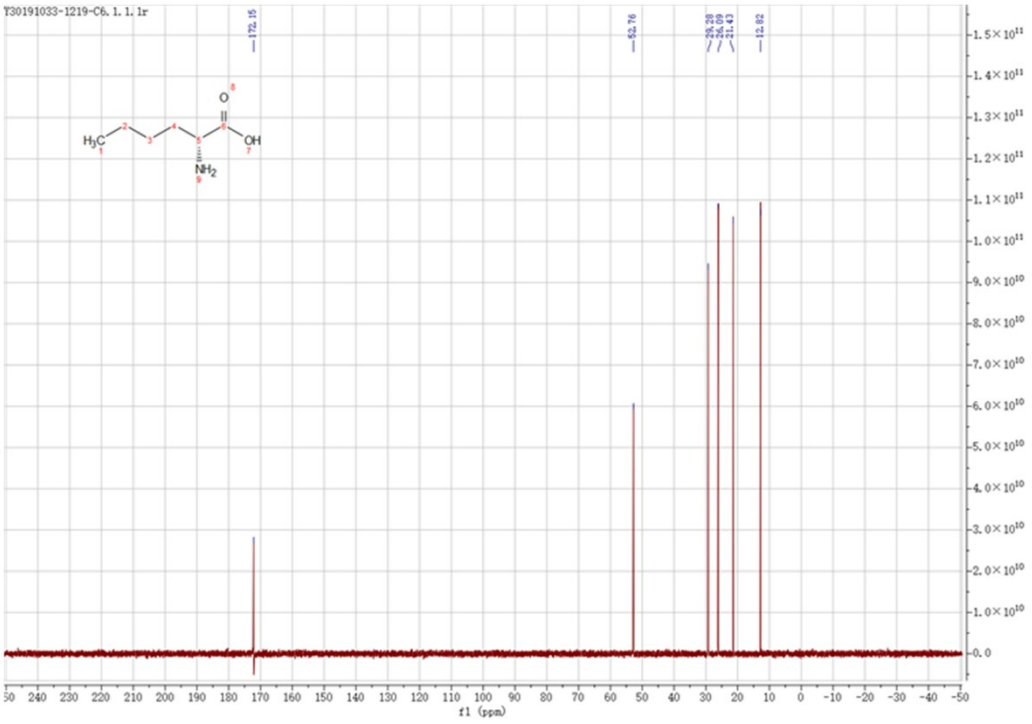

Fig. S21. ^{13}C NMR of isolated **1d** obtained from conversion of 10 mM **1a** by cascade.

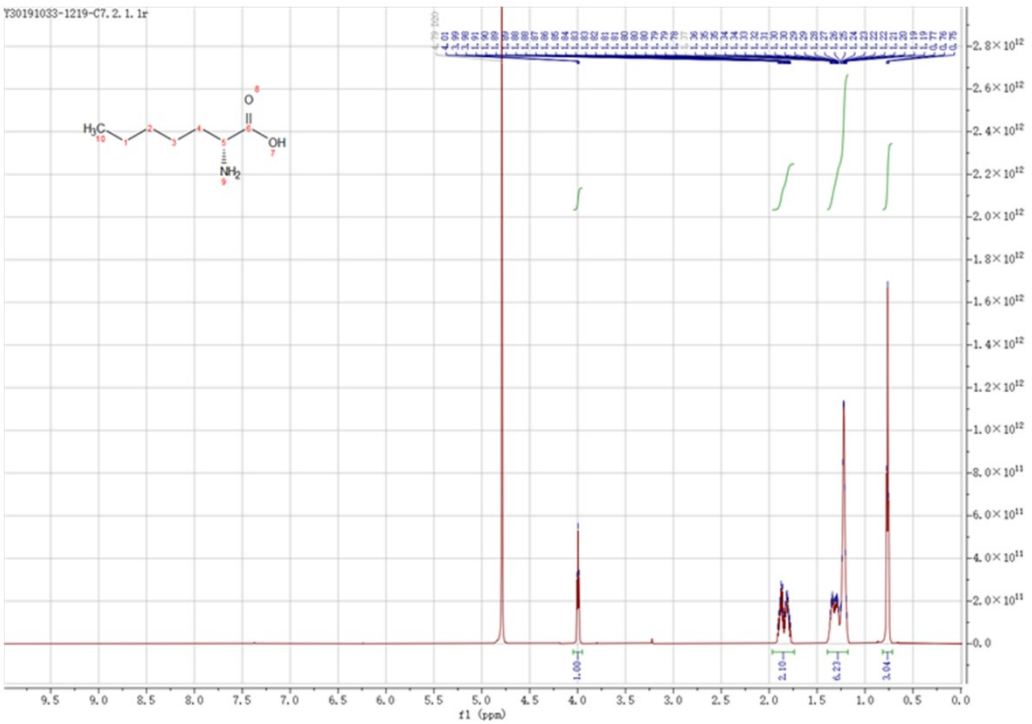

Fig. S22. ^{1}H NMR of isolated **2d** obtained from conversion of 10 mM **2a** by cascade.

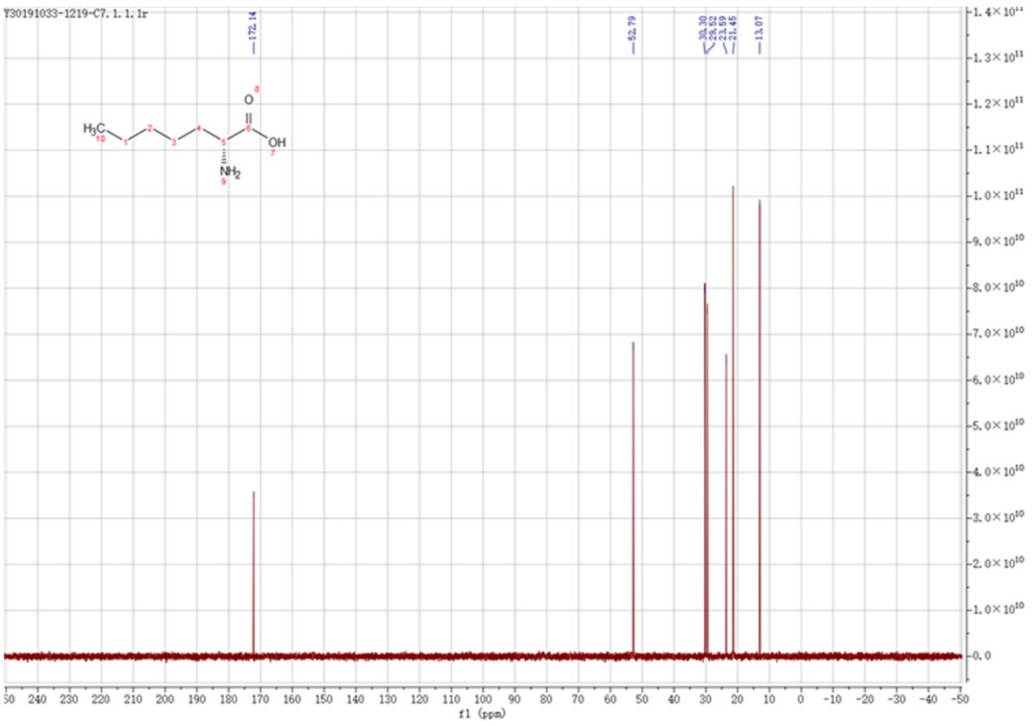

Fig. S23. ^{13}C NMR of isolated **2d** obtained from conversion of 10 mM **2a** by cascade.

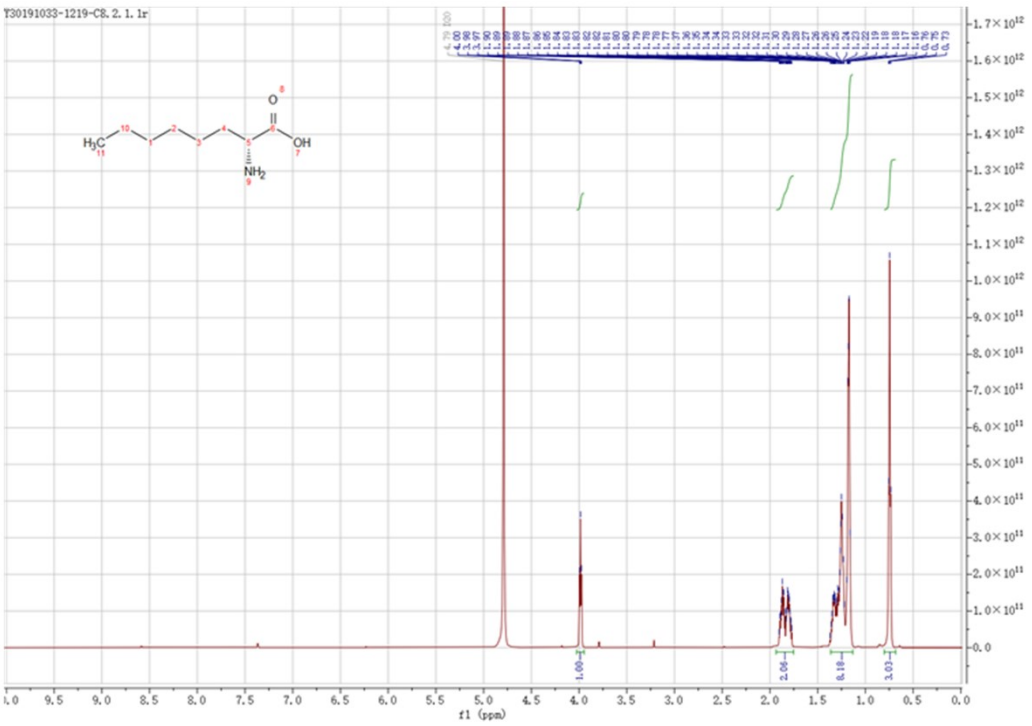

Fig. S24. ^{1}H NMR of isolated **3d** obtained from conversion of 10 mM **3a** by cascade.

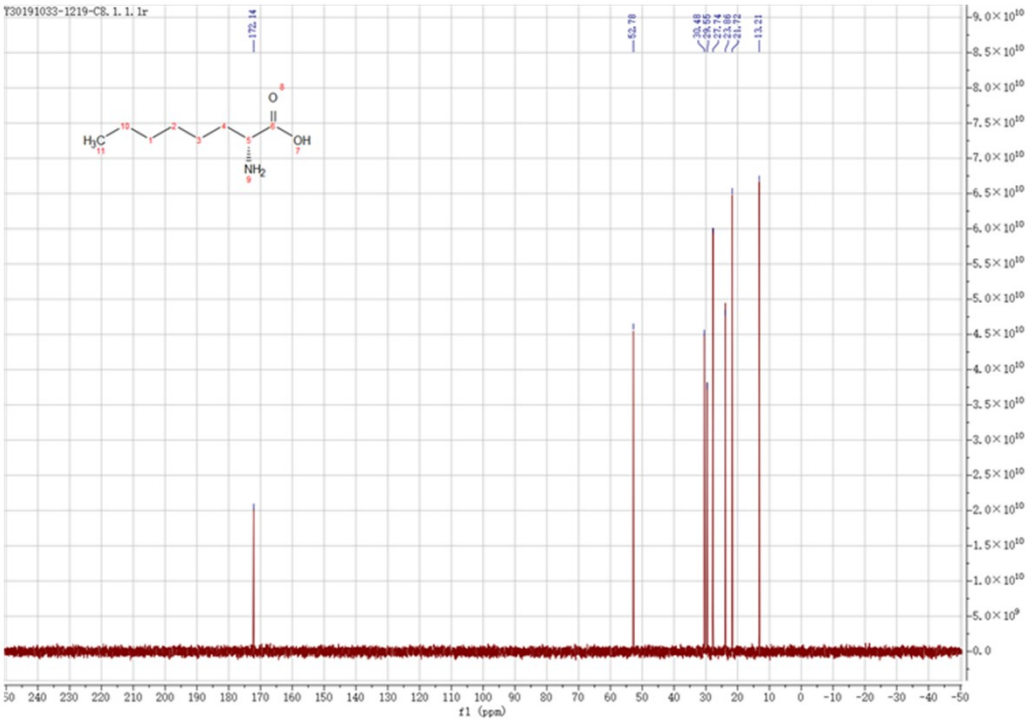

Fig. S25. ^{13}C NMR of isolated **3d** obtained from conversion of 10 mM **3a** by cascade.

References

[1] a) T. Omura, R. Sato, *J. Biol. Chem*. **1964**, 239, 2379-2385; b) T. Omura, R. Sato, J. Biol. Chem. **1964**, 239, 2370-2378.

[2] S. Gandomkar, A. Dennig, A. Dordic, L. Hammerer, M. Pickl, T. Haas, M. Hall, K. Faber, *Angew. Chem. Int. Ed.* **2017**, *57*, 427-430.

[3] a) C. B'Hymer, M. M. Bayon and J. A. Caruso, *J. Sep. Sci.* **2003**, 26, 7-19; b) R. Bhushan, H. Bruckner, *Amino Acids*, **2004**, 27, 231-247.

[4] a) H. Onoda, O. Shoji, K. Suzuki, H. Sugimoto, Y. Shiro, Y. Watanabe, *Catal. Sci. Technol*. **2018**, 8, 434-442; b) A. Dennig, F. Blaschke, S. Gandomkar, E. Tassano, B. Nidetzky, *Adv. Synth. Catal*. **2019**, 361, 1348-1358.

[5] A. Lopalco, G. Dalwadi, S. Niu, R. L. Schowen, J. Douglas, V. J. Stella, *J. Pharm. Sci*. **2016**, 105, 705-713.